

Novel High-Throughput Assay for Antioxidant Capacity against Superoxide Anion

LILIANG ZHANG,[†] DEJIAN HUANG,[‡] MIWAKO KONDO,[†] ELLEN FAN,[†]
 HONGPING JI,[§] YAN KOU,[§] AND BOXIN OU^{*†}

Brunswick Laboratories, Norton, Massachusetts 02766; Food Science and Technology Program, Department of Chemistry, National University of Singapore, Singapore 117543; and Brunswick Laboratories (China), 320, A3 Building, 218 Xing Hu Road, Suzhou Industrial Park, Suzhou, Jiangsu, China

A novel high-throughput assay for measuring antioxidant capacity against superoxide anion has been developed and validated. In this assay, hydroethidine (HE), a fluorescent probe, is oxidized by superoxide anion generated by xanthine and xanthine oxidase and increases its fluorescence intensity. Therefore, the inhibition of loss of HE's fluorescence intensity in the presence of antioxidant is an index of antioxidant capacity. The result is expressed as superoxide dismutase (SOD) equivalent. Unlike other probes, such as tetrazolium and lucigenin, one major advantage of this assay is that the use of HE is not prone to artifact. The method was rigorously validated through linearity, precision, accuracy, and ruggedness. The linear range, limit of quantitation (LOQ), and limit of detection (LOD) are 0.22–3.75 units/mL, 0.30 unit/mL, and 0.10 unit/mL, respectively. A wide variety of phenolic compounds and fruit extracts were analyzed.

KEYWORDS: Antioxidant activity; flavonoid; high throughput; hydroethidine; plate reader; SORAC; superoxide radicals

INTRODUCTION

Reactive oxygen species (ROS) are free radicals derived from molecular oxygen. They are essential in some cases such as the synthesis of thyroxine (1), the killing bacteria by phagocytosis (2), and normal cell signaling events (3). However, they can lead to free radical mediated chain reactions that indiscriminately target proteins (4), lipids (5), polysaccharides (6), and DNA (7). Among all of the ROS, superoxide anion ($O_2^{\cdot-}$), the product of one-electron reduction of oxygen, deserves much attention. Although it is not the strongest oxidant (the hydroxyl radical is much more reactive), it is the precursor of most ROS and a mediator in oxidative chain reactions. Therefore, foods containing antioxidants against superoxide anion will be the first line of defense against oxidative stress. An assay to assess antioxidant activity against $O_2^{\cdot-}$ of various natural products would provide a valuable tool to fight oxidative stress.

The existing methods used to determine the antioxidant activity against $O_2^{\cdot-}$ of small molecules, foods, or supplements are categorized into two types: nonspectrophotometric and spectrophotometric. Nonspectrophotometric methods include electron spin resonance spectroscopy (ESR) spin trapping (8) and pulse radiolysis (9). Spectrophotometric methods include

chemiluminescence (10) and absorbance (11). The existing methods are either not suitable for large-scale assessment or have some flaws derived from the assays' chemical principles. Therefore, a reliable high-throughput method for antioxidant activity scavenging $O_2^{\cdot-}$ is needed.

Here we present an accurate and highly efficient new assay to assess antioxidant capacity against $O_2^{\cdot-}$. We termed this new assay SORAC, standing for superoxide radical absorbance capacity. In the SORAC assay, xanthine and xanthine oxidase are used to produce superoxide anion (12). Hydroethidium (HE) is used as a fluorescence probe, and its oxidized product is monitored by fluorescence at $Ex = 480$ nm and $Em = 567$ nm (13). One of the advantages of this assay is the adoption of a high-throughput instrument platform. This platform consists of a multichannel liquid handling system online with a microplate fluorescence reader in a 96-well format (14). In addition to the vigorous validation of the SORAC assay, several flavonoids and fruit extracts were assessed for their superoxide radical scavenging capacity.

MATERIALS AND METHODS

Chemicals and Apparatus. Hydroethidine fluorescent stain was purchased from Polysciences, Inc. (Warrington, PA). Xanthine oxidase from buttermilk, xanthine, superoxide dismutase from bovine erythrocytes, and manganese(III) 5,10,15,20-tetra(4-pyridyl)-21H,23H-porphine chloride tetrakis(methochloride) were obtained from Sigma (St. Louis, MO). All phenolics including catechins ((+)-catechin, (-)-catechin gallate (CG), (-)-galliccatechin (GC), (-)-galliccatechin gallate (GCG), (-)-epicatechin (EC), (-)-epicatechin gallate (ECG), (-)-

* Address correspondence to this author at Brunswick Laboratories, 50 Commerce Way, Norton, MA 02766 [telephone (508) 285-2006, ext. 204; fax (508) 285-8002; e-mail bou@brunswicklabs.com].

[†] Brunswick Laboratories.

[‡] National University of Singapore.

[§] Brunswick Laboratories (China).

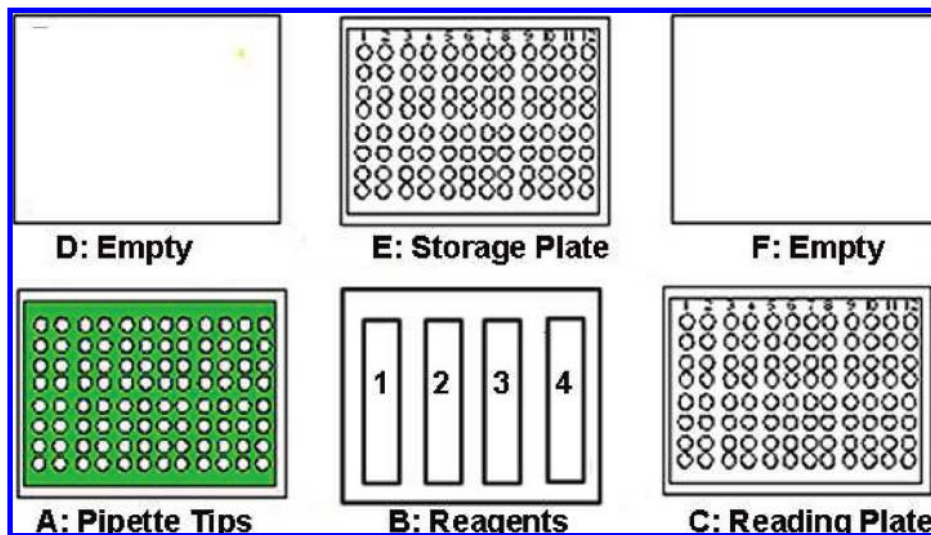


Figure 1. Layout of the deck of the Bio-Tek Precision 2000 showing the locations of stations.

epigallocatechin (EGC), and (–)-epigallocatechin gallate (EGCG) were also purchased from Sigma. Various analyzed samples were obtained “in house”.

An FL600 microplate fluorescence reader (Bio-Tek Instruments, Inc., Winooski, VT) was used with fluorescence filters for an excitation wavelength of 485 ± 20 nm and an emission wavelength of 590 ± 30 nm. The plate reader was controlled by software KC4 3.0 (revision 29). Sample dilution was accomplished by a Precision 2000 automatic pipetting system managed by precision power software (version 1.0) (Bio-Tek Instruments, Inc.). The 96-well polystyrene microplates and the covers were purchased from VWR International Inc. (Bridgeport, NJ).

Reagent and Standard Preparation. Three hundred milliliters of 75 mM phosphate buffer (pH 7.4) containing 100 μ M diethylenetriaminepentaacetic acid (DTPA) was made fresh on the day of use. This buffer solution was used to prepare the rest of the reagents and to dilute sample extracts. Ten milliliters of a 0.125 unit/mL xanthine oxidase solution was prepared in the buffer solution and kept in an ice bath. Xanthine solution was prepared by dissolving 0.015 g of xanthine in 5 mL of 0.1 N sodium hydroxide and 95 mL of the buffer. The mixed solution was sonicated for 10 min. This yielded 100 mL of xanthine solution. HE fluorescent stain stock solution (2 mg/mL) was prepared in acetonitrile. For each run, 20 mL of HE working solution (3.18 μ M) was prepared from the HE stock solution and the xanthine solution. Superoxide dismutase (SOD) stock solution (3000 units/mL) was prepared by dissolving 30000 units of SOD in 10 mL of the buffer solution. From the SOD stock solution, 10 mL of 30 units/mL SOD working solution was prepared by diluting the stock solution with the buffer solution and was kept in an ice bath. Manganese(III) 5,10,15,20-tetra(4-pyridyl)-21H,23H-porphine chloride tetrakis(methochloride) (0.02 g) was dissolved in 20 mL of the buffer solution to have an 1144 μ M manganese stock solution. Ten milliliters of manganese working solution was obtained by a 100 times dilution of the manganese stock solution with the buffer solution. This manganese working solution was used as a control.

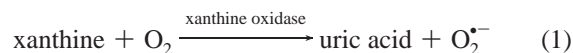
Sample Preparation. Flavonoids (see Table 2 for individual compounds) were directly dissolved in an acetone/water mixture (50:50, v/v) and diluted with 75 mM phosphate buffer (pH 7.4) for analysis. Various amounts of fruit samples were accurately weighed, and 20 mL of acetone/water (50:50, v/v) was added. The mixture was shaken at 400 rpm at room temperature on an orbital shaker for 1 h and then centrifuged at 25000g for 15 min. The supernatant was ready for analysis after appropriate dilution with the phosphate buffer solution containing 100 μ M DTPA.

Experimental Conditions. The automated sample preparation was performed using a Precision 2000 (14). The layout of the deck of the Bio-Tek Precision 2000 is illustrated in Figure 1. As shown, a 250 μ L pipet rack was placed at station A. Station B was the reagent vessel in which 20 mL of 75 mM phosphate buffer (pH 7.4) was added in reagent

holder 1 and 20 mL of 3.18 μ M hydroethidine was placed in reagent holder 2. A 96-well storage plate (maximum well volume = 320 μ L) was placed at station E for sample dilution, and in station C a reading plate was placed for the final solution. In the storage plate, 200 μ L of reagent was added manually into wells 1 and 12. Briefly, 200 μ L of 75 mM phosphate buffer (blank) was pipetted into wells A1, H1, A12, and H12. Two hundred microliters of SOD working solution was added to wells G1 and G12, and 200 μ L of manganese working solution was dispensed to wells D1 and D12. Then 200 μ L of eight different samples was dispensed into wells B1–F1 and B12–F12. The sample dilution sequence was programmed and controlled by the precision power software (version 1.10). Consecutive 1:2 dilutions were performed, and this would give a series of 1:2, 1:4, 1:8, 1:16, and 1:32 dilutions. Care was taken to ensure homogeneity of each dilution by thorough mixing at each stage through repeated aspiration and dispensing programmed by the precision power software.

A full automation of plate-to-plate liquid transfer was programmed. One hundred and fifty microliters of 3.18 μ M hydroethidine was pipetted into each well at station C. Then 25 μ L of diluted sample solution from each well of the storage plate was transferred into the corresponding reading plate well. Figure 2 illustrates the layout of the reading plate. The reading plate was covered with a lid and incubated for 20 min in a 37 °C oven. Twenty milliliters of xanthine oxidase was placed in reagent holder 4 at station B right after the incubation. The reading plate was then placed back to station C followed by the addition of 25 μ L of xanthine oxidase solution. The reading plate was immediately placed into the plate reader, and kinetic readings were taken every minute for 10 min.

Data Processing. The kinetic analysis of data was presented by Zhao et al. (13). $O_2^{\bullet-}$ is generated constantly by reaction 1 catalyzed by xanthine oxidase. The rate of superoxide production is constant and pseudozero order to the xanthine concentration, which is in large excess in comparison with the xanthine oxidase concentration.



The superoxide formed is either reacted with HE or scavenged by an antioxidant.



Dismutation of superoxide was not considered because at saturating concentrations of HE (compared to superoxide flux), this reaction is negligible (15).

	1	2	3	4	5	6	7	8	9	10	11	12
A	Blank	Blank	Blank	Blank	Blank	Blank	Blank	Blank	Blank	Blank	Blank	Blank
B	Sample 1 1	Sample 1 2	Sample 1 4	Sample 1 8	Sample 1 16	Sample 1 32	Sample 5 32	Sample 5 16	Sample 5 8	Sample 5 4	Sample 5 2	Sample 5 1
C	Sample 2 1	Sample 2 2	Sample 2 4	Sample 2 8	Sample 2 16	Sample 2 32	Sample 6 32	Sample 6 16	Sample 6 8	Sample 6 4	Sample 6 2	Sample 6 1
D	control 1	control 2	control 4	control 8	control 16	control 32	control 32	control 16	control 8	control 4	control 2	control 1
E	Sample 3 1	Sample 3 2	Sample 3 4	Sample 3 8	Sample 3 16	Sample 3 32	Sample 7 32	Sample 7 16	Sample 7 8	Sample 7 4	Sample 7 2	Sample 7 1
F	Sample 4 1	Sample 4 2	Sample 4 4	Sample 4 8	Sample 4 16	Sample 4 32	Sample 6 32	Sample 8 16	Sample 8 8	Sample 8 4	Sample 8 2	Sample 8 1
G	SOD 1	SOD 2	SOD 4	SOD 8	SOD 16	SOD 32	SOD 32	SOD 16	SOD 8	SOD 4	SOD 2	SOD 1
H	Blank	Blank	Blank	Blank	Blank	Blank	Blank	Blank	Blank	Blank	Blank	Blank

Figure 2. Layout of the 96-well microplate at station E: the number in each cell represents the sample dilution factor.

Assuming steady state concentration of $O_2^{\bullet -}$, the rate of superoxide consumption would be

$$-\frac{d[O_2^{\bullet -}]_1}{dt} = k_{HE}[HE]_1[O_2^{\bullet -}]_1 \quad \text{without an antioxidant} \quad (4)$$

$$-\frac{d[O_2^{\bullet -}]_2}{dt} = k_{HE}[HE]_2[O_2^{\bullet -}]_2 + k_{\text{antioxidant}}[\text{antioxidant}][O_2^{\bullet -}]_2 \quad \text{with an antioxidant} \quad (5)$$

In the above equations, HE is oversaturated, so its concentration in both cases should be the same ($[HE]_1 = [HE]_2 = [HE]$). Because the rate of superoxide consumption is determined only by the xanthine oxidase, the following equation should be true:

$$-\frac{d[O_2^{\bullet -}]_1}{dt} = -\frac{d[O_2^{\bullet -}]_2}{dt} \quad (6)$$

On the other hand, the fluorescence increase rates in the absence (V_1) and presence (V_2) of an antioxidant would be expressed as the following formulas:

$$V_1 = k_{HE}[HE][O_2^{\bullet -}]_1 \quad (7)$$

$$V_2 = k_{HE}[HE][O_2^{\bullet -}]_2 \quad (8)$$

From eqs 4–6, V_1 can be rewritten as

$$V_1 = k_{HE}[HE][O_2^{\bullet -}]_2 + k_{\text{antioxidant}}[\text{antioxidant}][O_2^{\bullet -}]_2 \quad (9)$$

Therefore, the fluorescence increase rates in the absence (V_1) and presence (V_2) of an antioxidant have the following relationship:

$$\frac{V_1}{V_2} = 1 + \frac{k_{\text{antioxidant}}[\text{antioxidant}]}{k_{HE}[HE]} \quad (10)$$

The plot of V_1/V_2 versus $[\text{antioxidant}]$ will give a linear function with an intercept at (0, 1) and a slope of $k_{\text{antioxidant}}/k_{HE}$. Figures 3 and 4 are the curves for SOD and Mn complex, respectively.

The slope $k_{\text{antioxidant}}$ is a reflection of SORAC. The larger the slope is, the higher the SORAC value would be. SOD was chosen as a

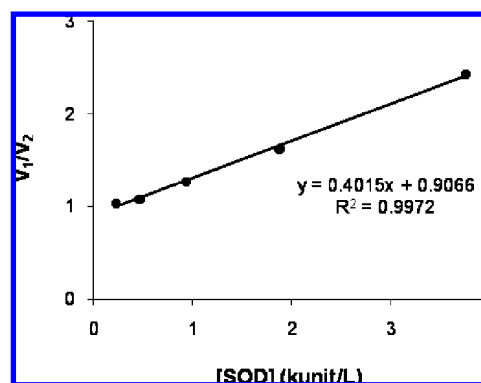


Figure 3. V_1/V_2 as a function of the concentration of SOD.

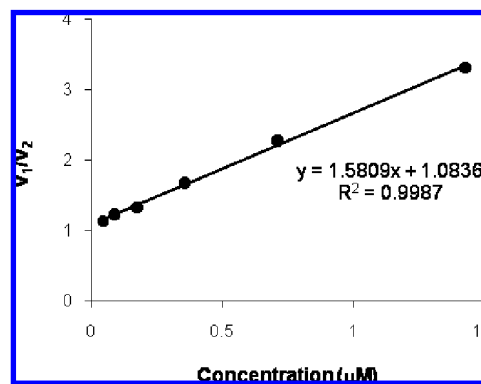


Figure 4. V_1/V_2 as a function of the concentration of manganese.

standard, and the individual sample's SORAC was defined as follows:

$$\text{SORAC} = k_{\text{sample}}/k_{\text{SOD}}$$

The unit of the SORAC would be units of SOD equivalents per gram (for solid) or units of SOD equivalents per liter (for liquid) depending on the form of the sample. This gives the SOD equivalent per gram or per liter of a sample.

RESULTS

Linearity. The linearity of the method was evaluated using SOD, phenolics, and fruit extracts at various concentrations. All analyzed samples showed a good linearity at various concentrations. The existence of a defined SORAC value itself

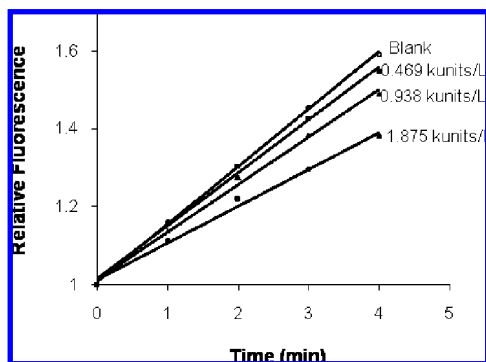


Figure 5. Relative fluorescence versus time (minutes) of reaction: blank and SOD at various concentrations.

Table 1. Linearity of SOD Standard Curve

run	slope	intercept	correl coeff
1	1.314	1.018	0.999
2	1.249	1.067	0.999
3	1.184	1.084	0.999
4	1.312	1.011	0.999
5	1.278	1.025	0.999
6	1.281	0.957	0.998
7	1.194	1.048	0.999
8	1.247	1.113	0.999
9	1.203	1.087	0.999
ave	1.251	1.046	N/A ^a
SD	0.049	0.048	N/A
CV%	3.933	4.590	N/A

^a Not applicable.

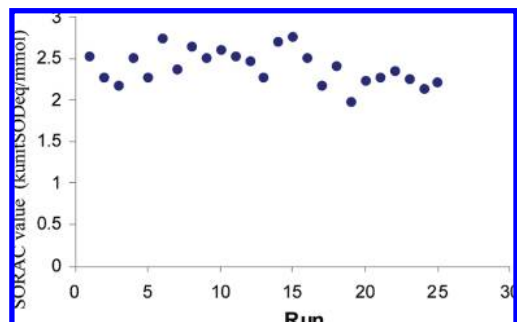


Figure 6. Ruggedness of SORAC assay determined by Mn complex (manganese(III) 5,10,15,20-tetra-(4-pyridyl)-21*H*,23*H*-porphine chloride, tetrakis(methochloride)).

demonstrated a very good linearity. **Figure 5** illustrates the hydroethidin fluorescence increment curves in the presence of SOD and xanthine oxidase. **Table 1** summarizes SOD linearity results: the average slope is 1.251 ± 0.049 , the correlation coefficient is >0.99 , and the intercept range is 1.046 ± 0.048 . The linearity range for SOD falls between 0.22 and 3.75 units/mL. The limit of quantitation (LOQ) and the limit of detection (LOD) are 0.30 and 0.10 unit/mL, respectively, using SOD as a calibration standard. **Table 2** shows the linear ranges for the analyzed samples.

Ruggedness of Assay. The reproducibility of the SORAC assay was evaluated by a ruggedness study using manganese(III) 5,10,15,20-tetra(4-pyridyl)-21*H*,23*H*-porphine chloride tetrakis(methochloride), an SOD mimic. Its activity was collected for 25 runs (**Figure 6**). The coefficient of variance (CV%) was 8.6. Therefore, the assay showed very good reliability.

SORAC Values of Antioxidants. To demonstrate the feasibility of the assay and obtain the structure relationships

Table 2. Linear Ranges of Fruit Extracts and Phenolic Compounds

sample	conc range (g/L)	R ²
Fruit Extracts		
bilberry powder	0.004–0.060	0.994
blackcurrant powder	0.004–0.028	0.996
blueberry powder	0.004–0.056	0.999
cranberry powder	0.089–0.710	0.992
grape seed extract	0.019–0.320	0.991
green tea polyphenols	0.003–0.015	0.991
raspberry powder	0.011–0.090	0.997
white tea extract	0.004–0.060	0.998
Phenolic Compounds		
caffeic acid	0.004–0.017	0.999
catechin (C)	0.008–0.064	0.991
catechin gallate (CG)	0.004–0.031	0.999
chlorogenic acid	0.005–0.040	0.999
epicatechin (EC)	0.016–0.130	0.999
epicatechin gallate (ECG)	0.004–0.031	0.995
epigallocatechin (EGC)	0.002–0.016	0.997
epicatechin gallate (ECG)	0.031–0.125	0.998
gallic acid	0.003–0.012	0.999
gallic acid ethyl ester	0.002–0.007	0.997
gallocatechin gallate (GCG)	0.003–0.013	0.999
rutin	0.020–0.080	0.999

Table 3. SORAC Values of Phenolic Compounds

compound	SORAC value ^a
caffeic acid	84.22 ± 3.44
C	22.45 ± 2.45
CG	74.28 ± 8.11
chlorogenic acid	20.06 ± 0.16
EC	49.67 ± 3.22
ECG	66.53 ± 16.79
EC	351.00 ± 26.64
EGCG	227.66 ± 25.41
gallic acid	336.90 ± 31.23
gallic acid ethyl ester	146.34 ± 13.25
GC	371.13 ± 11.91
GCG	202.54 ± 11.93
rutin	6.37 ± 0.48

^a SORAC values are expressed as units of SOD equivalent per gram ($n > 3$).

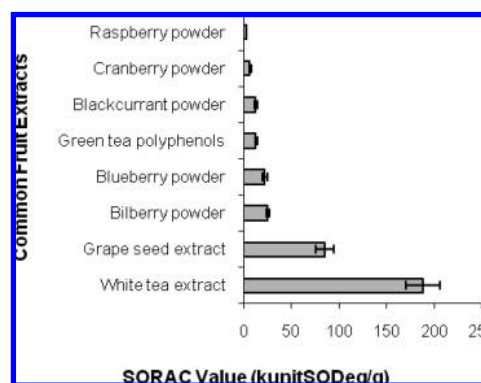


Figure 7. Rank order for superoxide radical scavenging capacity of fruit extracts based on the SORAC values.

with SORAC, we selectively examined some representative phenolic compounds, and the results are shown in **Table 3**. In addition, for the application purpose, we measured the SORAC values of fruit extracts as shown in **Figure 7**.

DISCUSSION

Problems Facing the Existing Methods. Although oxidation reactions are essential for life, they can also be harmful, causing oxidative stress and damaging cells. Even with the complex

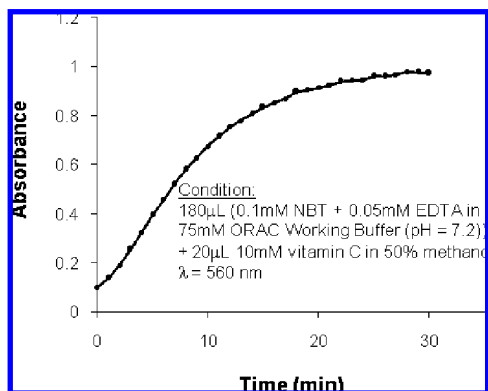


Figure 8. NBT reduction by ascorbic acid (vitamin C).

endogenous self-defense system against superoxide such as SOD (16), humans still need to take nonenzymatic antioxidants to better fight free radicals. Foods and supplements would be the common source of antioxidants. However, both current nonspectrophotometric and spectrophotometric methods retain drawbacks in selectivity, rapidity, cost performance, and convenience.

The most common nonspectrophotometric method is an assay using an ESR spin-trapping technique and tends to have cost and convenience problems. This method requires trapping agent and generally 5,5-dimethyl-1-pyrroline *N*-oxide (DMPO) is the one. The superoxide-trapping assay consumes a large volume of DMPO and makes the assay relatively expensive. Therefore, the ESR spin-trapping method is not suitable for a large-scale assessment. Moreover, an ESR machine is relatively expensive, and thus its broad applicability is limited.

Spectrophotometric methods, both absorbance and chemiluminescence, have a crucial problem, some flaws derived from assay principle. A system for spectrophotometric methods consists of a dye and a superoxide-generating source. Cytochrome *c* or nitroblue tetrazolium (NBT) is the major choice as a dye for absorbance assay to determine superoxide anion (11, 17, 18). The problem facing the cytochrome *c* assay is that the reduction of cytochrome *c* is a rather nonspecific reaction. Cytochrome *c* can be reduced by many reductive constituents present in foodstuffs and herbal supplements; thus, it is unsuitable for samples containing reducing compounds, such as vitamin C or other antioxidant compounds. In the case of NBT, its end product, diformazan, is not soluble in water. The precipitation can give variability in absorbance readings. Modified NBT derivatives are now commercially available that have water-soluble end-products: 3'-{1-[(phenylamino)-carbonyl]-3,4-tetrazolium}-bis(4-methoxy-6-nitro)benzenesulfonic acid hydrate (XTT), 4-[3-(4-iodophenyl)-2-(4-nitrophenyl)-2H-5-tetrazolio]-1,3-benzene disulfonate sodium salt (WST-1), and 4-[3-(2-methoxy-4-nitrophenyl)-2-(4-nitrophenyl)-2H-5-tetrazolio]-1,3-benzene disulfonate sodium salt (WST-8) (18–20). Although XTT overcame the issue associated with the end-product, it still holds some disadvantages (21). Because of the low water solubility, XTT requires heat to prepare a working solution, and the assay results are pH dependent. WST-1 and WST-8 were chosen as the replacements of NBT and XTT. WST overcame XTT's disadvantage by having higher water solubility, and the results are pH independent (21). Although the results produced by using WST are promising, the use of WST is still limited to biochemical samples. To our knowledge, there is no published result of the SOD assay using WST on botanical samples. In fact, NBT and XTT can be reduced by ascorbic acid and phenolic compounds to form formazans (Figure 8) (22); thus, the data lead to misinterpretation of results. On the basis of the

structure similarity among NBT derivatives listed above, there is a possibility that WST-1 and WST-8 can be reduced by phenolics as well.

Another spectrophotometric method, which is also commonly used, is the chemiluminescence method. As pointed out by Fridovich (23), this method is unreliable because $O_2^{\cdot-}$ can be mediated in the system by a chemiluminescent probe such as lucigenin or luminol (10, 24). $O_2^{\cdot-}$ is consumed by lucigenin radical, a reduced form of lucigenin, and the product of the reaction is decomposed with the emission of light for detection. Spontaneously, $O_2^{\cdot-}$ is produced as a result of lucigenin radical autoxidation. Therefore, the lucigenin radical acts as both $O_2^{\cdot-}$ generator and probe. Similarly, oxidized luminol reacts with $O_2^{\cdot-}$ to produce endoperoxide, which decomposes to aminophthalate accompanied by light emission, and oxidized luminol can reduce O_2 to $O_2^{\cdot-}$. Therefore, neither lucigenin nor luminol can count as a dependable probe to detect $O_2^{\cdot-}$ and is not suitable for the superoxide-scavenging assay.

As described above, up to now, there is no reliable published method to measure the scavenging capacity of $O_2^{\cdot-}$ for botanical samples. We here demonstrated that this fluorescence-based method using HE is specific to detect $O_2^{\cdot-}$, and can be used for botanical samples. Although HE can react with other reactive oxygen, nitrogen, and halogen species, only $O_2^{\cdot-}$ can oxidize HE into 2-hydroxyethidium (13, 25), resulting in an increase of fluorescence intensity. Hence, this makes HE an ideal probe in the SORAC assay. In addition, because the high-throughput instrument platform was applied to this method, we can run a number of samples in a short time while using less volume of solvents. Overall, the SORAC assay is a reliable high-throughput method for antioxidant activity scavenging $O_2^{\cdot-}$.

Relationship between Catechin Structures and SORAC.

In this study, we have tested various phenolic compounds including catechins. A structure–activity relationship was observed among catechins. Here we focus on catechins to overview the structural effects on SORAC.

Catechins are antioxidant polyphenols and are present in many foods and other plant species including teas, chocolates, and grapes. We have tested eight catechins shown in Figure 9. Their structures vary by epimers or by gallate ester groups or numbers of hydroxyl groups on the B-ring of the flavan skeleton. SORAC values of tested catechins are shown in Table 3.

Between *S*-epimers (C, CG, GC, and GCG) and *R*-epimers (EC, ECG, EGC, and EGCG), there is no significant difference in antioxidant activities. This indicates that sterical structure difference does not affect the SORAC values. In contrast, catechins with an additional hydroxyl group on C-5' of the B-ring (GC, EGC, GCG, and EGCG) were much more potent radical scavengers than others with no hydroxyl group on that position. This agreed with the results obtained by ESR (26), and it can be concluded that the structural importance of the additional hydroxyl group on C-5' for $O_2^{\cdot-}$ scavenging. In the condition of no hydroxyl group on C-5' of the B-ring, a galloyl moiety at C-3 of the C-ring enhances the superoxide scavenging activities (CG, ECG vs C, EC). Conversely, in the presence of a hydroxyl group on C-5' the activity of catechins with a galloyl moiety at C-3 on the C-ring (GCG and EGCG) was lower than that of catechins with no galloyl moiety at the position (GC and EGC). These inconsistent effects from a galloyl group cannot be explained. However, we can still conclude that a galloyl moiety is the important determinant of superoxide scavenging potential in the condition of no hydroxyl group on C-5' of the B-ring. As mentioned by Unno et al. (26), the radical scavenging effects are possibly due to ionization state, steric hindrance, and the stability of phenoxy radicals. In summary, the influence from

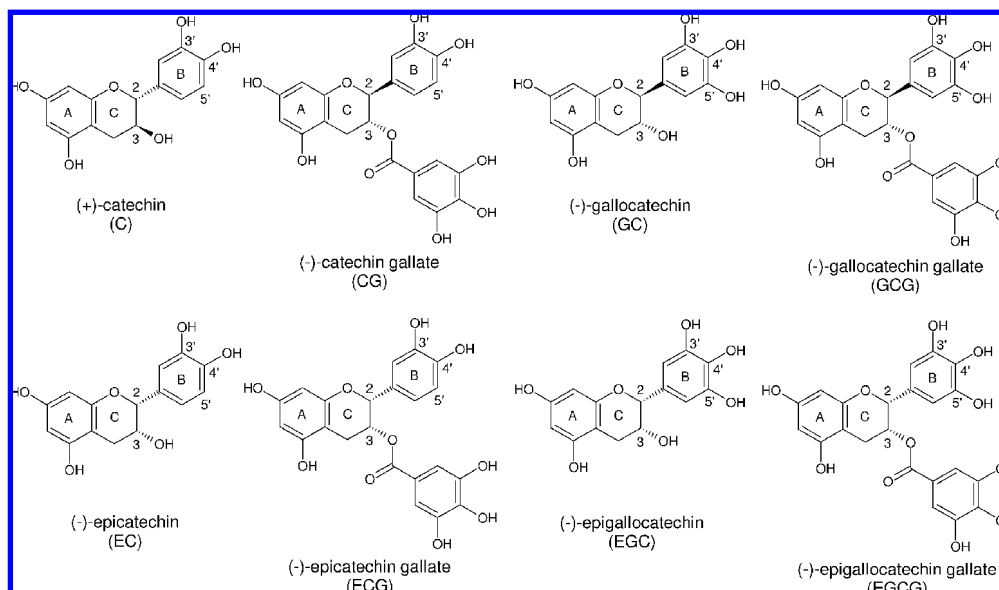


Figure 9. Structures of catechins.

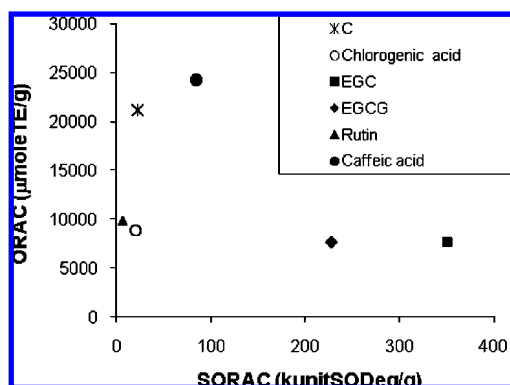


Figure 10. Correlation between SORAC expressed as units of SOD equivalents per gram (units SOD equiv/g) and ORAC (oxygen radical absorbance capacity) expressed as micromoles of Trolox equivalents per gram (μmol of TE/g).

an additional hydroxyl group and a galloyl moiety has been observed, but the sterical structure differences did not affect the SORAC of catechins.

Relation between ORAC and SORAC. The oxygen radical absorbance capacity (ORAC) assay is the method used to assess hydrophilic and lipophilic chain-breaking antioxidant capacity against peroxy radicals (14, 27). Using the ORAC, antioxidant capacity is measured by assessing the net area under the curve (AUC) from the AUC of a sample as compared to that of a blank. The AUC approach applies equally well for antioxidants that exhibit distinct lag phases and those samples that have no lag phases because both inhibition time and inhibition degree are measured as the reaction goes to completion. Therefore, the ORAC assay has been broadly applied in academia and the food and supplement industries as the method of choice to quantify antioxidant capacity. In a recent review, the ORAC assay is the most recommended method to quantify peroxy radical scavenging capacity (28). To comprehensively study different aspects of antioxidants, it is also suggested that different assays are needed, in addition to the ORAC assay. Figure 10 clearly indicates the necessity of the SORAC assay and different mechanisms between ORAC and SORAC.

In conclusion, we have developed a reliable, high-throughput assay for the determination of the antioxidant capacity against $\text{O}_2^{\cdot-}$. As a complement to the ORAC assay that is specific for

antioxidant capacity for peroxy radicals, the SORAC assay will be an important tool for quantitation of total antioxidant power against various ROS.

LITERATURE CITED

- (1) Rao, M. K.; Sagone, A. L., Jr. Extracellular metabolism of thyroid hormones by stimulated granulocytes. *Infect. Immun.* **1984**, *43*, 846–849.
- (2) Rosen, G. M.; Pou, S.; Ramos, C. L.; Cohen, M. S.; Britigan, B. E. Free radicals and phagocytic cells. *FASEB J.* **1995**, *9*, 200–209.
- (3) Dröge, W. Free radicals in the physiological control of cell function. *Physiol. Rev.* **2002**, *82*, 47–95.
- (4) Stadtman, E. R.; Levine, R. L. Protein oxidation. *Ann. N.Y. Acad. Sci.* **2000**, *899*, 191–208.
- (5) Rubbo, H.; Trostchansky, A.; Botti, H.; Batthyány, C. Interactions of nitric oxide and peroxynitrite with low-density lipoprotein. *Biol. Chem.* **2002**, *383*, 547–552.
- (6) Kaur, H.; Halliwell, B. Evidence for nitric oxide-mediated oxidative damage in chronic inflammation. Nitrotyrosine in serum and synovial fluid from rheumatoid patients. *FEBS Lett.* **1994**, *350*, 9–12.
- (7) Alexeyev, M. F.; Ledoux, S. P.; Wilson, G. L. Mitochondrial DNA and aging. *Clin. Sci. (London)* **2004**, *107*, 355–364.
- (8) Ueda, J.; Ikota, N.; Shinozuka, T.; Yamaguchi, T. Reactive oxygen species scavenging ability of a new compound derived from weathered coal. *Spectrochim. Acta A: Mol. Biomol. Spectrosc.* **2004**, *60*, 2487–2492.
- (9) Kono, Y.; Kobayashi, K.; Tagawa, S.; Adachi, K.; Ueda, A.; Sawa, Y.; Shibata, H. Antioxidant activity of polyphenolics in diets. Rate constants of reactions of chlorogenic acid and caffeic acid with reactive species of oxygen and nitrogen. *Biochim. Biophys. Acta* **1997**, *1335*, 335–342.
- (10) Tsai, C. H.; Chang, R. G.; Chiou, J. F.; Liu, T. Z. Improved superoxide-generating system suitable for the assessment of the superoxide-scavenging ability of aqueous extracts of food constituents using ultraweak chemiluminescence. *J. Agric. Food Chem.* **2003**, *51*, 58–62.
- (11) Chun, O. K.; Kim, D. O.; Lee, C. Y. Superoxide radical scavenging activity of the major polyphenols in fresh plums. *J. Agric. Food Chem.* **2003**, *51*, 8067–8072.
- (12) Fridovich, I. Quantitative aspects of the production of superoxide anion radical by milk xanthine oxidase. *J. Biol. Chem.* **1970**, *245*, 4053–4057.

- (13) Zhao, H.; Kalivendi, S.; Zhang, H.; Joseph, J.; Nithipatikom, K.; Vásquez-Vivar, J.; Kalyanaraman, B. Superoxide reacts with hydroethidine but forms a fluorescent product that is distinctly different from ethidium: potential implications in intracellular fluorescence detection of superoxide. *Free Radical Biol. Med.* **2003**, *34*, 1359–1368.
- (14) Huang, D.; Ou, B.; Hampsch-Woodill, M.; Flanagan, J. A.; Prior, R. L. High-throughput assay of oxygen radical absorbance capacity (ORAC) using a multichannel liquid handling system coupled with a microplate fluorescence reader in 96-well format. *J. Agric. Food Chem.* **2002**, *50*, 4437–4444.
- (15) Vásquez-Vivar, J.; Whittsett, J.; Martásek, P.; Hogg, N.; Kalyanaraman, B. Reaction of tetrahydrobiopterin with superoxide: EPR-kinetic analysis and characterization of the pteridine radical. *Free Radical Biol. Med.* **2001**, *31*, 975–985.
- (16) McCord, J. M.; Fridovich, I. Superoxide dismutase. An enzymic function for erythrocyte (hemocuprein). *J. Biol. Chem.* **1969**, *244*, 6049–6055.
- (17) Quick, K. L.; Hardt, J. I.; Dugan, L. L. Rapid microplate assay for superoxide scavenging efficiency. *J. Neurosci. Methods* **2000**, *97*, 139–144.
- (18) Peskin, A. V.; Winterbourn, C. C. A microtiter plate assay for superoxide dismutase using a water-soluble tetrazolium salt (WST-1). *Clin. Chim. Acta* **2000**, *293*, 157–166.
- (19) Sutherland, M. W.; Learmonth, B. A. The tetrazolium dyes MTS and XTT provide new quantitative assays for superoxide and superoxide dismutase. *Free Radical Res.* **1997**, *27*, 283–289.
- (20) Ukeda, H.; Shimamura, T.; Tsubouchi, M.; Harada, Y.; Nakai, Y.; Sawamura, M. Spectrophotometric assay of superoxide anion formed in Maillard reaction based on highly water-soluble tetrazolium salt. *Anal. Sci.* **2002**, *18*, 1151–1154.
- (21) Ukeda, H.; Kawana, D.; Maeda, S.; Sawamura, M. Spectrophotometric assay for superoxide dismutase based on the reduction of highly water-soluble tetrazolium salts by xanthine–xanthine oxidase. *Biosci. Biotechnol. Biochem.* **1999**, *63*, 485–488.
- (22) Vyas, D.; Sahoo, R.; Kumar, S. Possible mechanism and implications of phenolics-mediated reduction of XTT (sodium, 3'-[1-phenylaminocarbonyl]-3,4-tetrazolium]-bis(4-methoxy-6-nitro)benzene-sulfonic acid hydrate). *Curr. Sci.* **2002**, *83*, 1588–1592.
- (23) Fridovich, I. Editorial commentary on “Superoxide reacts with hydroethidine but forms a fluorescent product that is distinctly different from ethidium: potential implications in intracellular fluorescence detection of superoxide” by H. Zhao et al. *Free Radical Biol. Med.* **2003**, *34*, 1357–1358.
- (24) Taubert, D.; Breitenbach, T.; Lazar, A.; Censarek, P.; Harlfinger, S.; Berkels, R.; Klaus, W.; Roesen, R. Reaction rate constants of superoxide scavenging by plant antioxidants. *Free Radical Biol. Med.* **2003**, *35*, 1599–1607.
- (25) Zhao, H.; Joseph, J.; Fales, H. M.; Sokoloski, E. A.; Levine, R. L.; Vasquez-Vivar, J.; Kalyanaraman, B. Detection and characterization of the product of hydroethidine and intracellular superoxide by HPLC and limitations of fluorescence. *Proc. Natl. Acad. Sci. U.S.A.* **2005**, *102*, 5727–5732.
- (26) Unno, T.; Sugimoto, A.; Kakuda, T. Scavenging effect of tea catechins and their epimers on superoxide anion radicals generated by a hypoxanthine and xanthine oxidase system. *J. Sci. Food Agric.* **2000**, *80*, 601–606.
- (27) Ou, B.; Hampsch-Woodill, M.; Prior, R. L. Development and validation of an improved oxygen radical absorbance capacity assay using fluorescein as the fluorescent probe. *J. Agric. Food Chem.* **2001**, *49*, 4619–4626.
- (28) Huang, D.; Ou, B.; Prior, R. L. The chemistry behind antioxidant capacity assays. *J. Agric. Food Chem.* **2005**, *53*, 1841–1856.

Received for review October 24, 2008. Revised manuscript received January 9, 2009. Accepted February 3, 2009.

JF8033368